

See discussions, stats, and author profiles for this publication at: <https://www.researchgate.net/publication/264396330>

# Interaction between Formaldehyde and Luminescent MOF [Zn(NH<sub>2</sub>bdc)(bix)](n) in the Electronic Excited State

ARTICLE in THE JOURNAL OF PHYSICAL CHEMISTRY A · JULY 2014

Impact Factor: 2.69 · DOI: 10.1021/jp503722m · Source: PubMed

CITATIONS

5

READS

76

4 AUTHORS, INCLUDING:



**Xuedan Song**

Dalian University of Technology

18 PUBLICATIONS 130 CITATIONS

SEE PROFILE



**Jie Shan Qiu**

Dalian University of Technology

423 PUBLICATIONS 7,226 CITATIONS

SEE PROFILE



**Ce Hao**

Dalian University of Technology

134 PUBLICATIONS 919 CITATIONS

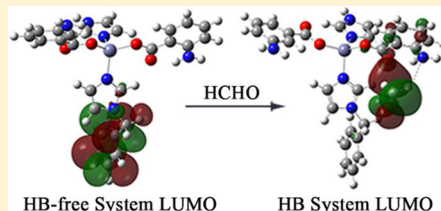
SEE PROFILE

# Interaction between Formaldehyde and Luminescent MOF $[\text{Zn}(\text{NH}_2\text{bdc})(\text{bix})]_n$ in the Electronic Excited State

Yuhang Yao, Xuedan Song, Jieshan Qiu, and Ce Hao\*

State Key Laboratory of Fine Chemicals, Dalian University of Technology, Dalian 116024, China

**ABSTRACT:** The hydrogen bond between formaldehyde and the luminescent metal–organic framework (MOF)  $[\text{Zn}(\text{NH}_2\text{bdc})(\text{bix})]_n$  was investigated using density functional theory and time-dependent density functional theory. The frontier molecular orbitals and electronic configuration demonstrate that the origin of the luminescence can be attributed to ligand-to-ligand charge transfer. Examination of the hydrogen bond behavior in the electronic excited state, with comparison of the electronic transition energies, bond distances, binding energy,  $^1\text{H}$ -NMR chemical shifts, and infrared spectra with those of the ground state, demonstrate that the hydrogen bond is stronger when in the electronic excited state. Strengthening of the hydrogen bond weakens the radioactive transition of  $[\text{Zn}(\text{NH}_2\text{bdc})(\text{bix})]_n$ , which thus leads to a luminescence decrease or quenching phenomenon, meaning that the luminescent MOF  $[\text{Zn}(\text{NH}_2\text{bdc})(\text{bix})]_n$  may be applied to the detection of formaldehyde.



## INTRODUCTION

Formaldehyde can act as an indoor air pollutant that strongly stimulates the eyes and respiratory system. It can also be considered carcinogenic and teratogenic, capable of inducing a variety of cancers.<sup>1,2</sup> For the detection of formaldehyde, Vairavamurthy et al. reviewed several in situ monitoring techniques, including differential optical absorption spectroscopy, laser-induced fluorescence spectroscopy, Fourier transform infrared spectroscopy, and tunable diode laser spectroscopy.<sup>2,3</sup> However, these traditional detection methods have some shortcomings, such as poor sensitivity, weak specificity, and long sampling times. In contrast, a new method that applies luminescent metal–organic frameworks (MOFs) as chemical sensor to indoor formaldehyde detection has attracted considerable attention because of its excellent features.<sup>4</sup> These excellent features of luminescent MOFs over other materials and methods is a consequence of several key elements, such as the visible signal change to the naked eye and the single molecule level detection limits,<sup>5</sup> the combination of synthetic flexibility with respect to both the organic and inorganic components,<sup>6</sup> high surface areas, and structural flexibility.<sup>5,6</sup> Another virtue is that the tenability of MOFs sorption properties offers a high degree of molecular specificity, and their large surface areas combined with confinement of the analyte inside the MOFs cavities can potentially translate to high sensitivity.<sup>5,6</sup> Recently, Yan et al. have made a thorough inquiry in the geometric and electronic structures of host–guest interactions in the crystal interior with periodic density functional theoretical (DFT), and some significant experiments indicated that the electronic structures and energy transfer processes in the luminescence can influence the optical properties; hence, these host–guest systems have potential applications as fluorescence sensors.<sup>7–9</sup> Formaldehyde can form hydrogen bond with luminescent MOFs, significantly affecting the luminescent properties of the luminescent

MOFs.<sup>6,10,11</sup> Therefore, for formaldehyde, luminescent MOFs may be considered a type of potential chemical sensor with the high sensitivity, high selectivity, fast response time, and high stability.<sup>5,11–13</sup>

Wen et al. recently synthesized a MOF  $[\text{Zn}(\text{NH}_2\text{bdc})(\text{bix})]_n$  (where  $\text{NH}_2\text{bdc}$  = 2-amino-1,4-benzenedicarboxylic acid and  $\text{bix}$  = 1,4-bis(imidazol-1-ylmethyl) benzene) that possesses a three-dimensional structure with a 5-fold interpenetrating 4-connected net and that luminesces at 426 nm.<sup>14</sup> The strength of the luminescence exhibited by this system would increase, and the luminescence wavelength would be altered when the MOF interacts with a variety of small molecules.<sup>14</sup> Therefore, this type of MOF may prove useful as a potential chemical sensor for detecting formaldehyde in the air.

Hydrogen bond is the main noncovalent interaction exhibited between molecular and supramolecular systems.<sup>10</sup> Consequently, the behavior of the hydrogen bond in the electronically excited state is closely related to the luminescence properties of these materials.<sup>10,11</sup> Lately, the change of MOF properties due to the formation of hydrogen bond and its behavior in the electronic excited state were noticed.<sup>10,15–18</sup> Some time-dependent (TD)DFT calculations have been performed to examine the relationship between the fluorescence properties and the formation of hydrogen bonds.<sup>10,11,18</sup>

In this work, the hydrogen bond between the luminescent MOF  $[\text{Zn}(\text{NH}_2\text{bdc})(\text{bix})]_n$  and formaldehyde was considered. We have analyzed the frontier molecular orbitals (MOs) and electron configuration in the ground state to confirm the origin of the luminescence of  $[\text{Zn}(\text{NH}_2\text{bdc})(\text{bix})]_n$ . We then studied the behavior of the hydrogen bond in the electronic excited state by comparing the geometries, binding energy, nuclear

Received: April 16, 2014

Revised: July 23, 2014

Published: July 28, 2014

magnetic resonance, and infrared spectra of the hydrogen bonded complexes of the ground and excited states. Finally, the possibility of employing  $[\text{Zn}(\text{NH}_2\text{bdc})(\text{bix})]_n$  as a detector of formaldehyde was discussed.

## ■ COMPUTATIONAL DETAILS

**Computational Model.** A suitable finite representative fragment of  $[\text{Zn}(\text{NH}_2\text{bdc})(\text{bix})]_n$  was obtained from the periodic structure for use in calculations (complex 1, see Figure 1a). Complex 1, containing a Zn ion, two  $\text{NH}_2\text{bdc}$

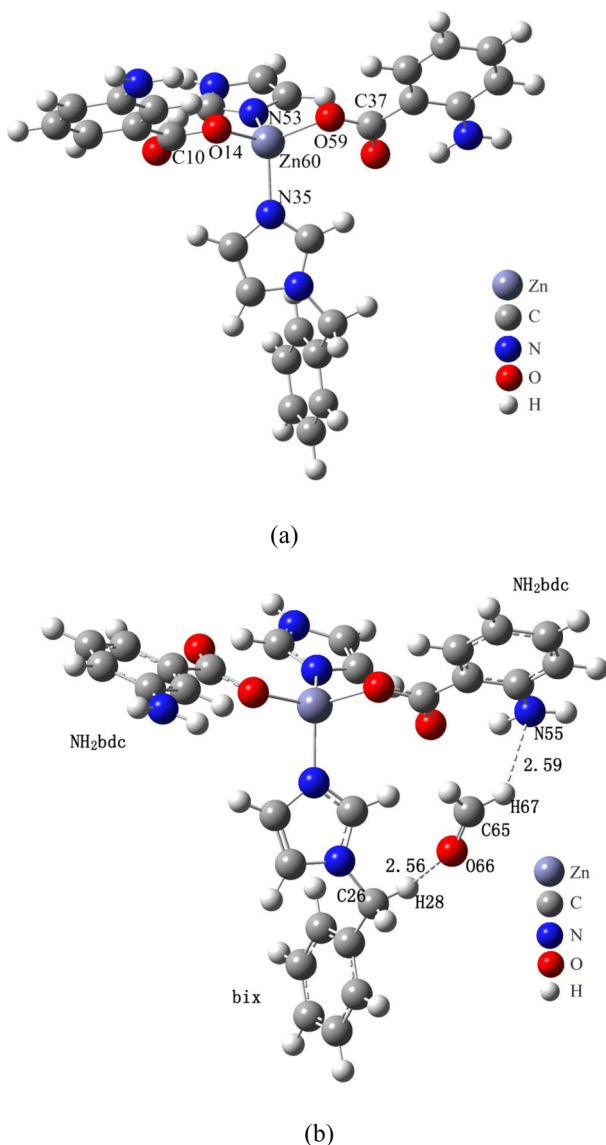


**Figure 1.** Computational Models. (a) Representative fragment complex 1. (b) Hydrogen bond complex model complex 2.

ligands, and two  $\text{bix}$  ligands (of which one is without its benzene ring), was saturated with hydrogen atoms to obtain the representative fragment.

To study the effect of hydrogen bond on the luminescent properties of  $[\text{Zn}(\text{NH}_2\text{bdc})(\text{bix})]_n$ , we then added a formaldehyde molecule to model complex 1 to obtain the hydrogen-bonded (HB) model complex 2 (Figure 1b). Complex 2 was the most stable DFT-optimized geometry of 13 possible HB complexes considered. In complex 2, one hydrogen bond was

formed between H67 of formaldehyde and N55 of complex 1, while another was formed by O66 of formaldehyde and H28 of complex 1. The locations and distances of these two hydrogen bonds, as well as some other important atoms and ligands, are illustrated in Figure 1b, where the dotted lines represent the hydrogen bonds.

**Computational Methods.** The geometries, vibrational frequencies, binding energy, and electronic transition energies of complex 1 and complex 2 were calculated using DFT and TDDFT with the hybrid exchange-correlation functional CAM-B3LYP and LANL2DZ basis sets.<sup>19–22</sup> The ground state and excited state IR spectra were calculated and scaled by 0.961 (NIST Computational Chemistry Comparison and Benchmark Database, NIST Standard Reference Database Number 101, Release 15b, August 2011, Editor Russell D. Johnson III; <http://cccbdb.nist.gov/>) using the optimized ground state and excited state structures, respectively.<sup>23–25</sup> The UV/vis spectrum and fluorescent emission spectrum were calculated using the functional BVP86 and the 6-31++G basis sets. For the NMR calculations we used the functional CAM-B3LYP and the 6-311++G(d, p) basis sets.<sup>21–23</sup> All quantum chemical calculations were carried out using the Gaussian 09 suite of programs.<sup>19</sup> In addition, the electronic configurations were calculated using the ADF2012 program by employing the B3LYP hybrid functional and DZ basis sets.

The binding energy was calculated with the basis set superposition error (BSSE) correction:  $E_{\text{binding}} = E_{\text{complex2}} - E_{\text{HCHO}} - E_{\text{complex1}} + E_{\text{BSSE}}$ .<sup>16,17</sup>

## ■ RESULTS AND DISCUSSION

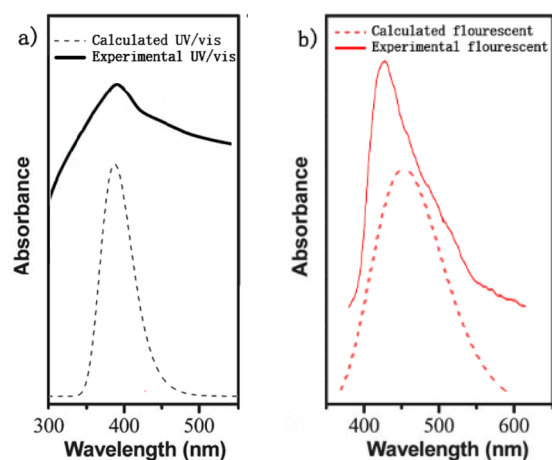
**Structure Optimization.** The calculated optimized geometry parameters and vibrational frequencies of complex 1 are in good agreement with those obtained by experiment (Table 1).<sup>14</sup> In addition, the calculated UV–vis spectrum with the maximum absorption band at 388 nm is consistent with the experimental value 390 nm, and the computational fluorescent emission spectrum with the maximum absorption band at 454 nm is also close to the experimental spectrum (maximum absorption at 426 nm) (Figure 2).<sup>14</sup> Therefore, we can say that the structural fragment used provides a credible representation of the periodic system.

**Frontier Molecular Orbitals and Electronic Configuration.** Molecular orbital (MO) analysis can provide direct insight into the nature of the excited state.<sup>26</sup> In principle, on the basis of Kasha's rule, other excited states that are higher in energy would quickly deactivate to the lowest vibration levels of the  $S_1$  state. Photon emission only occurs in appreciable yield from the lowest excited state of a given multiplicity.<sup>27</sup> Therefore, herein, we only discuss the lowest excited state ( $S_1$ ) and the ground state ( $S_0$ ).

From the calculated frontier MOs, we can see that the electron density distribution of the highest occupied molecular orbital (HOMO) and lowest unoccupied molecular orbital (LUMO) of complex 1 are mostly localized on the  $\text{NH}_2\text{bdc}$  ligand and  $\text{bix}$  ligand (Figure 3a). In addition, the electron density distributions of the HOMO and LUMO of complex 2 are mainly localized on the  $\text{NH}_2\text{bdc}$  ligand and formaldehyde (Figure 3b). Comparison of the frontier MOs in complex 1 and complex 2 reveals that the hydrogen bonds significantly alter the LUMO of the MOF  $[\text{Zn}(\text{NH}_2\text{bdc})(\text{bix})]_n$ . These changes can lead to the transfer of electron and energy from MOF to formaldehyde in the electronic excited states. Several previous works of Yan et al. have reported that the occurrence of energy

**Table 1.** Calculated Geometric Parameters and Experimental Values of Complex 1

bond	the geometric optimization (Å)	experimental values (Å) <sup>a</sup>
O14–Zn60	1.96	2.09
O59–Zn60	1.96	1.97
N35–Zn60	2.06	1.91
N53–Zn60	2.06	1.95
O14–C10	1.31	1.24
O59–C37	1.31	1.24
bond angles	the geometric optimization (deg)	experimental values (deg) <sup>a</sup>
O59–Zn60–O14	113	95
O59–Zn60–N35	111	111
O59–Zn60–N53	107	111
O14–Zn60–N35	108	106
O14–Zn60–N53	112	113
N35–Zn60–N53	106	119
dihedral angles	the geometric optimization (deg)	experimental values (deg) <sup>a</sup>
O14–Zn60–O59–C37	171	171
O14–Zn60–N35–C31	28	23
vibration frequencies	the geometric optimization (cm <sup>−1</sup> )	experimental values (cm <sup>−1</sup> ) <sup>a</sup>
ν(N–H)	3388	3428
ν(C–H)	3142	3325
ν(amino benzene acid skeleton)	1639, 1309	1670, 1365
ν(ligands skeleton)	1510	1576
ν(amino benzene acid O–C)	1368	1438
ν(imidazole N–C)	1050	1093
r(benzene C–H)	776, 728	831, 772

<sup>a</sup>Reference 14.**Figure 2.** Comparison of (a) experimental (ref 14) and computational UV–vis spectra and (b) experimental (ref 14) and computational fluorescent emission spectra for luminescent MOF [Zn(NH<sub>2</sub>bdc)(bix)]<sub>n</sub>.

transfer from MOF host to guest molecules can selectively change the luminescence behavior of luminescent MOF.<sup>7,9</sup> Therefore, the formation of hydrogen bonds between formaldehyde and [Zn(NH<sub>2</sub>bdc)(bix)]<sub>n</sub> would change the luminescence properties of the MOF.

Wen et al. have attributed the luminescence of [Zn(NH<sub>2</sub>bdc)(bix)]<sub>n</sub> to ligand-to-metal charge transfer (LMCT) due to the broad peak at 426 nm of MOF and broad emission ( $\lambda_{\text{max}} = 551 \text{ nm}$ ) of ligand NH<sub>2</sub>bdcH<sub>2</sub>.<sup>14</sup> However, a study of

Yan et al. revealed that the energy blocking action of the Zn<sup>2+</sup> cation may confine the valence electrons localized in ligand effectively; as a result, there is no energy or electron transfer that occurs between the ligand and the Zn atom during the fluorescence process, then the MOF presents blue-shifted emission and enhanced photoluminescence quantum yield.<sup>8</sup> This presentation is consistent with the luminescent behavior of the MOF [Zn(NH<sub>2</sub>bdc)(bix)]<sub>n</sub> and ligand NH<sub>2</sub>bdcH<sub>2</sub>. Therefore, we have reason to suspect the luminescence mechanism of the MOF cannot attribute to LMCT.

To reveal the luminescence mechanism of the MOF [Zn(NH<sub>2</sub>bdc)(bix)]<sub>n</sub>, electronic configuration can provide direct insight into the nature of luminescence. The electronic configuration of complex 1 (Figure 3a) indicates that the HOMO is composed of p orbitals of the C and N atoms of the NH<sub>2</sub>bdc ligand and that the LUMO is composed of p orbitals of benzyl C atoms of the bix ligand. The HOMO of complex 2 (Figure 3b) is composed of p orbitals of the C and N atoms of the NH<sub>2</sub>bdc ligand, and the LUMO is composed of p orbitals of the C and O atoms of formaldehyde. Analysis of the frontier MOs and electronic configuration demonstrate that the origin of the luminescence exhibited by [Zn(NH<sub>2</sub>bdc)(bix)]<sub>n</sub> can be attributed to ligand-to-ligand charge transfer (LLCT), which differs from the LMCT proposed by Wen et al. for this system.<sup>14</sup>

**Electronic Transition Energies.** The calculated electronic transition energies of complex 2 are lower than those of complex 1 (Table 2). Hydrogen bond influences the process of electronic excitation, leading to an alteration in the charge distribution in the hydrogen bond complex in different electronic states.<sup>28,29</sup> The calculated results are consistent with the rules summarized by Zhao et al., in which enhancement of hydrogen bonds in the S<sub>1</sub> state reduces the electronic transition energies, resulting in a red shift in the electronic spectra.<sup>10,26,30</sup>

Monitoring changes in the electronic transition energy can, therefore, predict the behavior of the excited state hydrogen bonds. On the basis of the calculations presented, strengthening of the hydrogen bonds in the S<sub>1</sub> state can be inferred, and this behavior could further affect the luminescence properties.<sup>31</sup>

**Hydrogen Bonds Behavior in the S<sub>1</sub> State.** The strength of a hydrogen bond can be evaluated by four aspects, namely, the hydrogen bond distance, the binding energy, the chemical shift of the hydrogen atom involved, and the characteristic vibrational frequencies of the chemical bonds close to the hydrogen bonds.

The length of the hydrogen bond between H67 and N55 decreased from 2.59 Å in the S<sub>0</sub> state to 1.89 Å in the S<sub>1</sub> state, and the length of the hydrogen bond between H28 and O66 decreased from 2.58 Å in the S<sub>0</sub> state to 2.14 Å in the S<sub>1</sub> state (Table 3). Moreover, the binding energy decreased from −21.0 kJ/mol in S<sub>0</sub> state to −25.6 kJ/mol in S<sub>1</sub> state. This reveals that the two hydrogen bonds were strengthened when the system went from the S<sub>0</sub> state to the S<sub>1</sub> state.

The <sup>1</sup>H-NMR chemical shift of the hydrogen atom involved in hydrogen bond can also be used to monitor the hydrogen bond strength.<sup>32</sup> When the hydrogen bond is strengthened, the distance between the hydrogen atom and electronegative atom (N55 or O66) is decreased, meaning that the charge density around the nucleus of the hydrogen is increased. This leads to enhanced shielding and an upfield shift in the chemical shift.<sup>10</sup> The H67 chemical shift, i.e., of the atom involved in the hydrogen bonds formation, decreased from 21.4 ppm in the S<sub>0</sub>



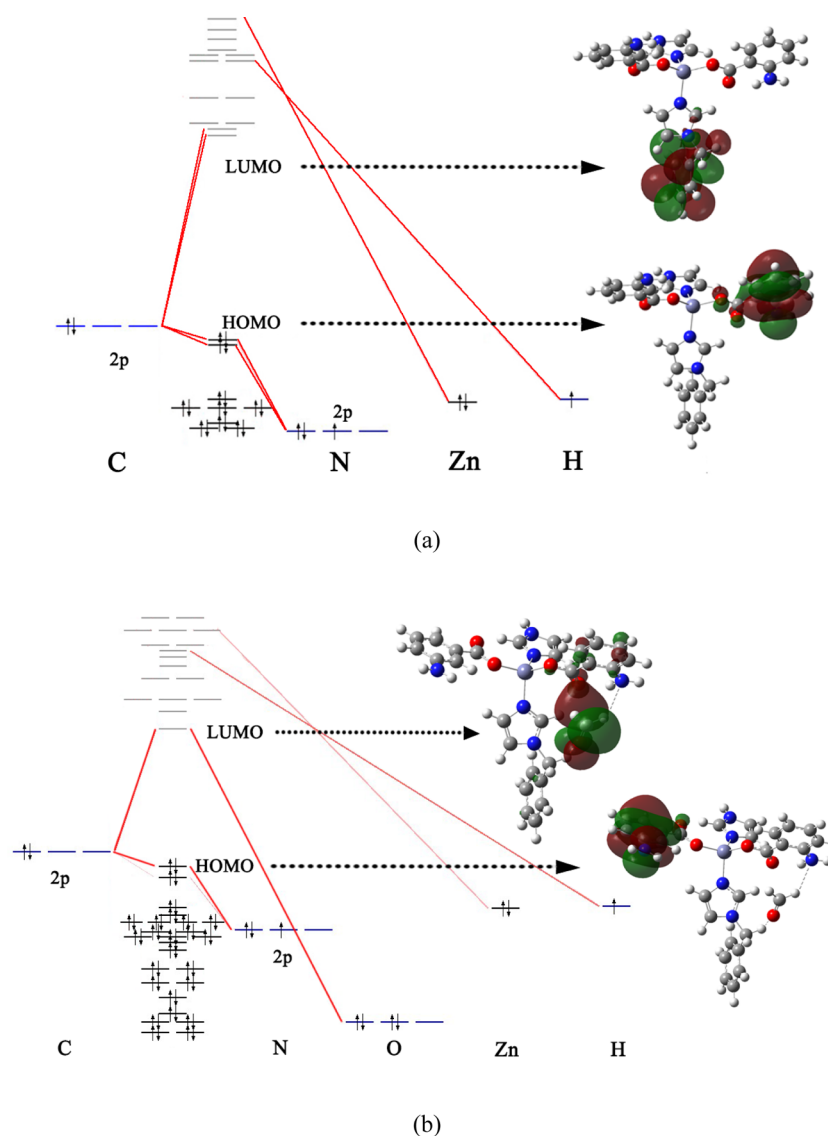


**Figure 3.** (a) The frontier orbitals and electron configuration of complex 1. (b) The frontier orbitals and electron configuration of complex 2.

**Table 2. Electronic Transition Energies of Complexes 1 and 2**

excited states	complex 1 (eV)	complex 2 (eV)
$S_1$	2.68	1.86
	H $\rightarrow$ L <sup>a</sup> 70.7%	H $\rightarrow$ L <sup>a</sup> 70.7%
$S_2$	2.71	2.19
$S_3$	2.79	2.46
$S_4$	2.82	2.83
$S_5$	3.11	2.86
$S_6$	3.15	2.95
$S_7$	3.29	3.01
$S_8$	3.30	3.16
$S_9$	3.33	3.18
$S_{10}$	3.34	3.21

<sup>a</sup>H, HOMO; L, LUMO.

state to 17.9 ppm in the  $S_1$  state (Table 3). Additionally, the chemical shift of H28 decreased from 26.0 ppm in the  $S_0$  state to 23.6 ppm in the  $S_1$  state (Table 3). All of these shifted upfield, meaning that the two hydrogen bonds strength were enhanced going from the  $S_0$  state to the  $S_1$  state, which is

**Table 3. Hydrogen Bond Length and  $^1\text{H}$ -NMR Chemical Shift in the  $S_0$  State and  $S_1$  State of Complex 2**

bond length (Å)	$S_0$	$S_1$
H67...N55	2.59	1.89
H28...O66	2.58	2.14
$^1\text{H}$ -NMR (ppm)	$S_0$	$S_1$
H67	21.4	17.9
H28	26.0	23.6
binding energy (kJ/mol)	−21.0	−25.6

consistent with the conclusion drawn from examination of the changes in bond distances and binding energy.

The strength of hydrogen bond can be described by changes in characteristic frequencies of chemical bonds close to the hydrogen bonds.<sup>10,33</sup> The red shift of the characteristic vibrational frequencies of the  $S_1$  state illustrate the enhancement of the hydrogen bonds from the  $S_0$  state.<sup>10,33</sup>

We also examined the characteristic vibrational stretching frequencies of the chemical bonds that are in close proximity to the hydrogen bonds, including C65=O66, C65–H67, and C26–H28, to describe the behavior of the hydrogen bonds in

the  $S_1$  state. The stretching frequency of the C65=O66 chemical bond decreased from 1662  $\text{cm}^{-1}$  in the  $S_0$  state to 1318  $\text{cm}^{-1}$  in the  $S_1$  state (Figure 4a), and the C65–H67

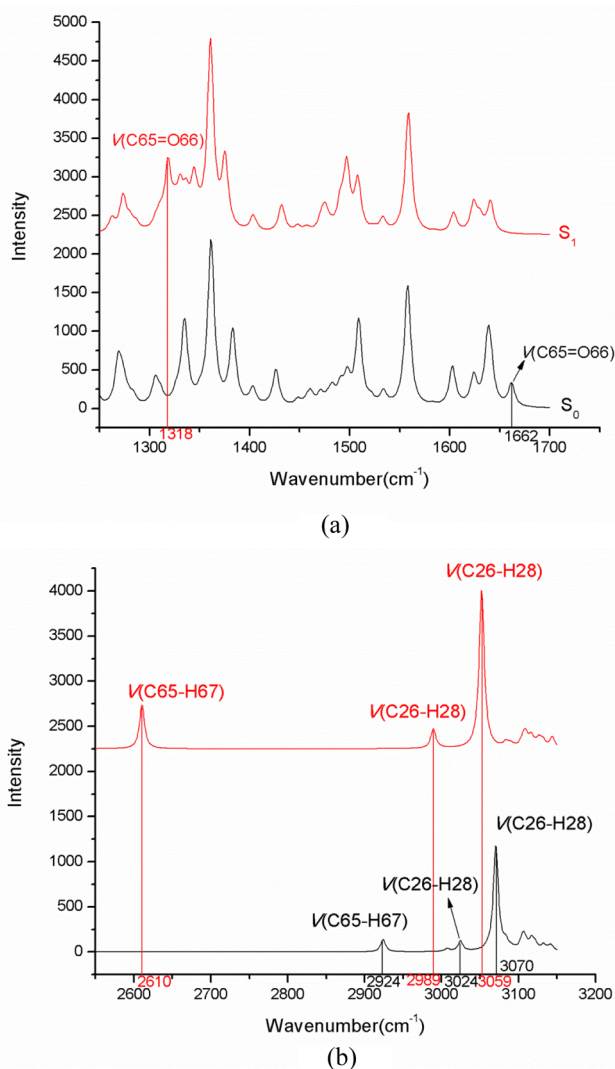


**Figure 4.** (a) Stretching vibration frequency of C65=O66. (b) Stretching vibration frequency of C65–H67 and C26–H28.

stretching frequency decreased from 2924  $\text{cm}^{-1}$  in the  $S_0$  state to 2610  $\text{cm}^{-1}$  in the  $S_1$  state (Figure 4b). Furthermore, the asymmetric stretching frequency associated with the C26–H28 of a methylene decreased from 3070  $\text{cm}^{-1}$  ( $S_0$ ) to 3059  $\text{cm}^{-1}$  ( $S_1$ ), while the symmetric stretch associated with this group decreased from 3024  $\text{cm}^{-1}$  ( $S_0$ ) to 2989  $\text{cm}^{-1}$  ( $S_1$ ) (Figure 4b). All of these characteristic stretching frequencies are red-shifted when going from the  $S_0$  to  $S_1$  state, with these shifts also proving that the two hydrogen bonds are stronger in the  $S_1$  state compared with the  $S_0$  state.<sup>10,33</sup>

#### Effect of Hydrogen Bonds on Luminescent Properties.

The discussion on the behavior of hydrogen bonds in the  $S_1$  state demonstrated that the hydrogen bonds of complex 2 is enhanced in the  $S_1$  state. The strengthening of the hydrogen bonds can also decrease the energy gap between the  $S_0$  state and  $S_1$  state. In other words, the electronic transition energies of complex 2 are lower than those of complex 1 as a result of the formation of hydrogen bonds.

In this work, the HB-free complex system corresponded to the HB-free system shown in Figure 5; only complexes

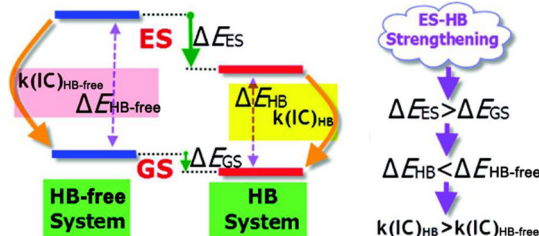


**Figure 5.** Schematic view of the enhancement of internal conversion (IC) by excited-state hydrogen bond strengthening behavior. Reprinted with permission from ref 6. Copyright 2012 American Chemical Society.

corresponding to the HB system in Figure 5 were considered. The stronger hydrogen bonds in the  $S_1$  state causes a larger downshift of the excited state energy level than that in the  $S_0$  state ( $\Delta E_{ES} > \Delta E_{GS}$ ). As a result, the energy gap between the  $S_1$  and  $S_0$  state of the HB system would decrease more than that of the HB-free system ( $\Delta E_{HB} > \Delta E_{HB-free}$ ). Electronic coupling between the  $S_1$  state and  $S_0$  state is strengthened, thereby increasing the rate of nonradioactive transition. Because nonradioactive transition is a competitive process to radioactive transition, the strengthening of the hydrogen bonds is not favorable to radioactive transition. Therefore, according to the energy gap law, the rate of internal conversion (IC) from the  $S_1$  state to  $S_0$  state is enhanced ( $k(IC)_{HB} > k(IC)_{HB-free}$ ). Thus, internal conversion is the most important dissipative process for the  $S_1$  state.<sup>34</sup> This is consistent with rules summarized by Zhao et al.<sup>10,15</sup> and some other recent progress.<sup>11,18</sup>

The enhanced hydrogen bonds in the  $S_1$  state promotes a decrease in luminescence or quenching phenomenon, and it is not favorable to the luminescent behavior of  $[\text{Zn}(\text{NH}_2\text{bdc})(\text{bix})]_n$ . As a result, in theory, it is possible to detect formaldehyde using  $[\text{Zn}(\text{NH}_2\text{bdc})(\text{bix})]_n$ .

## CONCLUSIONS

In this work, the representative fragment complex 1 was truncated from the periodic structure for use in calculations. Analysis of the frontier orbitals and electron configuration reveals that the origin of the luminescence is LLCT, rather than LMCT as was previously proposed. Comparison of the electronic transition energies, bond distances, binding energy,  $^1\text{H}$ -NMR chemical shifts, and infrared spectra in the  $S_0$  and  $S_1$  states indicate that the hydrogen bonds are stronger in the excited state. Moreover, hydrogen bonds strengthening in the  $S_1$  state leads to a decrease in luminescence or quenching phenomenon of  $[\text{Zn}(\text{NH}_2\text{bdc})(\text{bix})]_n$ . Therefore, it can be expected that the luminescent properties of MOFs could be controlled by tuning hydrogen bonds.  $[\text{Zn}(\text{NH}_2\text{bdc})(\text{bix})]_n$  may be used as a detector of formaldehyde. Furthermore, our studies have also shown that a fragment approach to explore the luminescent behavior of MOFs can be credible.

## AUTHOR INFORMATION

### Corresponding Author

\*(C.Hao) E-mail: haoce@dlut.edu.cn. Phone: +86-411-84986335. Fax: +86-411-84748086.

## Notes

The authors declare no competing financial interest.

## ■ ACKNOWLEDGMENTS

We acknowledge the financial support of the National Natural Science Foundation of China (Grants 21373042, 21036006, and 21137001), the Fundamental Research Funds for the Central Universities (Grant No. 1001852005), and the Dalian Scientific Program (No. 2011A15GX023).

## ■ REFERENCES

- (1) Peder, W.; Gunnar, D. N. Non-cancer Effects of Formaldehyde and Relevant for Setting an Indoor Air Guideline. *Environ. Int.* **2010**, *36*, 788–799.
- (2) Salthammer, T.; Mentese, S.; Marutzky, R. Formaldehyde in the Indoor Environment. *Chem. Rev.* **2010**, *110*, 2536–2572.
- (3) Vairavamurthy, A.; Roberts, J. M.; Newman, L. Methods for Determination of Low-Molecular-Weight Carbonyl-Compounds in the Atmosphere. *Atmos. Environ.* **1992**, *26A*, 1965–1993.
- (4) Kawamura, K.; Kerman, K.; Fujihara, M.; Nagatani, N.; Hashiba, T.; Tamiya, E. Development of a Novel Hand-held Formaldehyde Gas Sensor for the Rapid Detection of Sick Building Syndrome. *Sens. Actuators, B* **2005**, *105*, 495–501.
- (5) Kreno, L. E.; Leong, K.; Farha, O. K.; Allendorf, M.; Van Duyne, R. P.; Hupp, J. T. Metal-Organic Framework Materials as Chemical Sensors. *Chem. Rev.* **2012**, *112*, 1105–1125.
- (6) Allendorf, M. D.; Bauer, C. A.; Bhakta, R. K.; Houk, R. J. Luminescent Metal-Organic Frameworks. *Chem. Soc. Rev.* **2009**, *38*, 1330–1352.
- (7) Yan, D. P.; Tang, Y. Q.; Lin, H. Y.; Wang, D. Tunable Two-color Luminescence and Host-guest Energy Transfer of Fluorescent Chromophores Encapsulated in Metal-Organic Frameworks. *Sci. Rep.* **2014**, *4*, 4337–4343.
- (8) Yan, D. P.; Gao, R.; Wei, M.; Li, S. D.; Lu, J.; Evans, D. G.; Duan, X. Mechanochemical Synthesis of a Fluorenone-based Metal Organic Framework with Polarized Fluorescence: an Experimental and Computational Study. *J. Mater. Chem. C* **2013**, *1*, 997–1004.
- (9) Yan, D. P.; Lloyd, G. O.; Delori, A.; Jones, W.; Duan, X. Tuning Fluorescent Molecules by Inclusion in a Metal–Organic Framework: An Experimental and Computational Study. *ChemPlusChem* **2012**, *77*, 1112–1118.
- (10) Zhao, G. J.; Han, K. L. Hydrogen Bonding in the Electronic Excited State. *Acc. Chem. Res.* **2012**, *45*, 404–413.
- (11) Sui, X.; Mi, W.; Ji, M.; Hao, C.; Qiu, J. Hydrogen Bonding and Coordination Bond in the Electronically Excited States of the MOF  $\text{Cu}_2(\text{L})_2$  ( $\text{L} = 5\text{-(4-pyridyl)tetrazole}\cdot\text{CH}_2\text{Cl}_2$ ): A Time-Dependent Density Functional Theory Study. *J. Lumin.* **2013**, *142*, 110–115.
- (12) Cui, Y.; Li, A. J.; Li, B.; Ma, X.; Bai, R.; Zhang, W.; Ren, M. S.; Sun, J. Microstructure and Ablation Mechanism of C/C-SiC Composites. *J. Eur. Ceram. Soc.* **2014**, *34*, 171–177.
- (13) Qiu, S.; Zhu, G. Molecular Engineering for Synthesizing Novel Structures of Metal-Organic Frameworks with Multifunctional Properties. *Coord. Chem. Rev.* **2009**, *253*, 2891–2911.
- (14) Wen, L.; Zhou, L.; Zhang, B.; Meng, X.; Qu, H.; Li, D. Multifunctional Amino-decorated Metal-Organic Frameworks: Non-linear-optic, Ferroelectric, Fluorescence Sensing and Photocatalytic Properties. *J. Mater. Chem.* **2012**, *22*, 22603–22609.
- (15) Zhao, G. J.; Han, K. L. Site-Specific Solvation of the Photoexcited Protochlorophyllide *a* in Methanol: Formation of the Hydrogen-Bonded Intermediate State Induced by Hydrogen-Bond Strengthening. *Biophys. J.* **2008**, *94*, 38–46.
- (16) Yang, D. P.; Yang, Y. G.; Liu, Y. F. Effects of Different-Type Intermolecular Hydrogen Bonds on the Geometrical and Spectral Properties of 6-Aminocoumarin Clusters in Solution. *Commun. Comput. Chem.* **2013**, *1*, 205–215.
- (17) Zhang, M. X.; Mi, W. H.; Hao, C. Theoretical Study on a Metal-Organic Framework Based on  $\mu_4$ -oxo Tetrazinc Clusters: the Sorption Mechanism for Small Molecules. *Commun. Comput. Chem.* **2013**, *1*, 269–281.
- (18) Sui, X.; Ji, M.; Lan, X.; Mi, W.; Hao, C.; Qiu, J. Role of the Electronically Excited-State Hydrogen Bonding and Water Clusters in the Luminescent Metal-Organic Framework. *Inorg. Chem.* **2013**, *52*, 5742–5748.
- (19) Becke, A. D. Density-Functional Thermochemistry. III. The Role of Exact Exchange. *J. Chem. Phys.* **1993**, *98*, 5648–5652.
- (20) Perdew, J. P. Density Functional Approximation for the Correlation Energy of the Inhomogeneous Electron Gas. *Phys. Rev. B* **1986**, *33*, 8822–8824.
- (21) Yanai, T.; Tew, D. P.; Handy, N. C. A New Hybrid Exchange-correlation Functional using the Coulomb-Attenuating Method (CAM-B3LYP). *Chem. Phys. Lett.* **2004**, *393*, 51–57.
- (22) Frisch, M. J.; Trucks, G. W.; Schlegel, H. B.; Scuseria, G. E.; Robb, M. A.; Cheeseman, J. R.; Scalmani, G.; Barone, V.; Mennucci, B.; Petersson, G. A.; et al. *Gaussian 09*, revision A.02; Gaussian, Inc.: Wallingford, CT, 2009.
- (23) Hay, P. J.; Wadt, W. R. Ab Initio Effective Core Potentials for Molecular Calculations. Potentials for the Transition Metal Atoms Sc to Hg. *J. Chem. Phys.* **1985**, *82*, 270–283.
- (24) Hay, P. J.; Wadt, W. R. Ab Initio Effective Core Potentials for Molecular Calculations. Potentials for K to Au including the Outermost Core Orbitals. *J. Chem. Phys.* **1985**, *82*, 299–310.
- (25) Wadt, W. R.; Hay, P. J. Ab Initio Effective Core Potentials for Molecular Calculations. Potentials for Main Group Elements Na to Bi. *J. Chem. Phys.* **1985**, *82*, 284–298.
- (26) Wu, D. Y.; Mi, W. H.; Ji, M.; Hao, C. The Effect of Furcated Hydrogen Bonding and Coordination Bond on Luminescent Behavior of Metal-Organic Framework [CuCN·EIN]: a TDDFT Study. *Spectrochim. Acta, Part A* **2012**, *97*, 589–593.
- (27) Kasha, M. Characterization of Electronic Transitions in Complex Molecules. *Discuss. Faraday Soc.* **1950**, *9*, 14–19.
- (28) Wen, L.; Dang, D. B.; Duan, C. Y.; Li, Y. Z.; Tian, Z. F.; Meng, Q. J. 1D Helix, 2D Brick-Wall and Herringbone, and 3D Interpenetration  $d^{10}$  Metal-Organic Framework Structures Assembled from Pyridine-2,6-dicarboxylic Acid N-Oxide. *Inorg. Chem.* **2005**, *44*, 7161–7160.
- (29) Zhao, G. J.; Liu, J. Y.; Zhou, L. C.; Han, K. L. Site-Selective Photoinduced Electron Transfer from Alcoholic Solvents to the Chromophore Facilitated by Hydrogen Bonding: A New Fluorescence Quenching Mechanism. *J. Phys. Chem. B* **2007**, *111*, 8940–8945.
- (30) Zhao, G. J.; Han, K. L. Effects of Hydrogen Bonding on Tuning Photochemistry: Concerted Hydrogen-Bond Strengthening and Weakening. *ChemPhysChem* **2008**, *9*, 1842–1846.
- (31) Liu, Y. F.; Ding, J. X.; Liu, R. Q.; Shi, D. H.; Sun, J. F. Historical Biogeography of the Genus *Chamaecyparis* (Cupressaceae, Coniferales) Based on Its Fossil Record. *J. Photochem. Photobiol., A* **2009**, *201*, 203–209.
- (32) Zhao, G. J.; Northrop, B. H.; Stang, P.; Han, K.-L.; Stang, P. J. The Effect of Intermolecular Hydrogen Bonding on the Fluorescence of a Bimetallic Platinum Complex. *J. Phys. Chem. A* **2010**, *114*, 9007–9013.
- (33) Zhao, G. J.; Han, K. L. Early Time Hydrogen-Bond Dynamics of Photoexcited Coumarin 102 in Hydrogen-Donating Solvents: Theoretical Study. *J. Phys. Chem. A* **2007**, *111*, 2469–2474.
- (34) Englman, R.; Jortner, J. The Energy Gap Law for Radiationless Transitions in Large Molecules. *Mol. Phys.* **1970**, *18*, 145–164.